α+Li and H+Be decay of ^{10,11,12}B

N. Curtis,[1,*] N. I. Ashwood,[1] W. N. Catford,[1] N. M. Clarke,[1] M. Freer,[1] D. Mahboub,[2] C. J. Metelko,[1,†] S. D. Pain,[2,‡] N. Soić,[1,§] and D. C. Weisser[3]

[1]*School of Physics and Astronomy, University of Birmingham, Edgbaston, Birmingham, B15 2TT, United Kingdom*

[2]*School of Electronics and Physical Sciences, University of Surrey, Guildford, Surrey, GU2 7XH, United Kingdom*

[3]*Department of Nuclear Physics, Research School of Physical Sciences and Engineering, Australian National University, Canberra, ACT, 0200, Australia*

(Received 13 June 2005; published 31 October 2005)

A study of the α+^{6}Li, α+^{6}Li*, d+^{8}Be and p+^{9}Be decay of ^{10}B, the α+^{7}Li, t+^{8}Be, and d+^{9}Be decay of ^{11}B and the α+^{8}Li and t+^{9}Be decay of ^{12}B has been performed using the ^{12}C(^{7}Li,^{10}B*)^{9}Be, ^{16}O(^{7}Li,^{10}B*)^{13}C, ^{7}Li(^{7}Li,^{11}B*)t, and ^{7}Li(^{7}Li,^{12}B*)d reactions at 58 MeV. The excitation energy of the ^{10,11,12}B* was determined following the coincident detection of the α+Li and H+Be decay fragments. A study of the relative yields for the decay of a number of excited states in ^{10,11,12}B* indicates that the α-decay channel dominates in all cases.

DOI: 10.1103/PhysRevC.72.044320 PACS number(s): 21.10.−k, 23.60.+e, 27.20.+n

I. INTRODUCTION

In recent years, there has been considerable interest in the structure of light neutron-rich nuclei at, or near, the neutron drip line. To understand the properties of these exotic nuclei, it is crucial that the structure of the near-stability isotopes and the evolution of this structure toward the limits of stability are fully understood. One example is that of the boron isotopic chain. Ground state cluster structures of ^{4}He+^{11}Li, ^{6}He+^{11}Li, and ^{8}He+^{11}Li have been predicted for ^{15}B, ^{17}B, and ^{19}B, respectively, following antisymmetrized molecular dynamics calculations of the ground state properties of ^{11,13,15,17,19}B by Kanada-En'yo and Horiuchi [1]. To test these predictions, the cluster structure of the near-stability boron isotopes must be studied in detail to provide a foundation for measurements closer to the drip line.

Recently, a number of studies of the charged particle decay and cluster structure of ^{10,11,12}B have been reported [2–7]. These include the p, d, and α decay of ^{10}B and the α decay of ^{11}B and ^{12}B. In a study of the ^{7}Li(^{12}C,^{10}B*)^{9}Be reaction at 76 MeV, Leask *et al.* [2] observed that the α+^{6}Li$_{gs}$ decay of ^{10}B dominates over the p+^{9}Be, d+^{8}Be, and α+^{6}Li* [2.185 MeV, 3^{+}] channels, suggesting that the α+^{6}Li configuration plays an important role in the structure of this nucleus. Two previously unreported $T = 0$ states at (7.96 ± 0.07) and (9.58 ± 0.06) MeV were also seen in the α+^{6}Li* [2.185 MeV, 3^{+}] channel. Evidence supporting the existence of the 7.96 MeV state was also obtained by Soić *et al.* [3] in the α+^{6}Li*[2.185 MeV, 3^{+}] channel following a measurement of the ^{9}Be(^{7}Li,^{10}B*)^{6}He reaction at 52 MeV.

More recently, Ahmed *et al.* [4] employed a 302 MeV ^{10}Be fragmentation beam and the ^{12}C(^{10}Be,^{10,11}B*) reaction to study the α decay of both ^{10}B and ^{11}B at the Grand Accelerateur National D'Ions Lourds (GANIL), France. The α+^{6}Li decay of ^{10}B was observed from states at 5.2, 6.1, and (6.5) MeV (in agreement with [2]), and the α+^{7}Li decay of ^{11}B from states at 9.3 and 10.3 MeV. The α decay of ^{11}B has also been studied following d pickup onto a ^{9}Be beam in the ^{7}Li(^{9}Be,^{11}B*)^{5}He reaction [5,6]. In this work, the α+^{7}Li$_{gs}$ breakup of ^{11}B was observed from many states in the 9–19 MeV excitation energy region. The strong observation of α decay above the n, p, d, and t decay thresholds (together with the well known α+t cluster structure of ^{7}Li) was seen as an indication of an α-cluster structure for these states, proposed to be of an α+α+t nature.

The first observation of the α+^{8}Li decay of ^{12}B was reported recently by Soić *et al.* [3,7] from states at (10.5), 10.9, 11.6, 13.4, (14.1), 15.7, and (17.7) MeV. The 15.7 MeV state was proposed as a possible candidate for a three-center α+α+t structure with one valence neutron, analogous to the proposed α+α+α+n structure for the 11.08 MeV state in ^{13}C [8]. Further studies [5] have confirmed the α decay of these states.

In this paper, we report on a study of the ^{12}C(^{7}Li,^{10}B*)^{9}Be, ^{16}O(^{7}Li,^{10}B*)^{13}C, ^{7}Li(^{7}Li,^{11}B*)t, and ^{7}Li(^{7}Li,^{12}B*)d reactions performed at a beam energy of 58 MeV. The first measurements of the relative decay strengths for the α+^{6}Li, p+^{9}Be, d+^{8}Be, and α+^{6}Li*[2.185 MeV, 3^{+}] decay of ^{10}B, the α+^{7}Li, t+^{8}Be, and d+^{9}Be decay of ^{11}B, and the α+^{8}Li and t+^{9}Be decay of ^{12}B for individual states will be presented. The most likely mechanism for the population of the states is a sequential (two-step) breakup reaction. For example, the ^{7}Li(^{7}Li,α ^{7}Li)t channel probably proceeds via an initial two-body ^{7}Li(^{7}Li,^{11}B*)t α-transfer reaction which is followed by a sequential decay of ^{11}B* to α+^{7}Li. It is noted, however, that the measurement of the branching ratios is independent of the reaction mechanism populating the states.

II. EXPERIMENTAL DETAILS

The experiment was performed at the 14 UD tandem Van de Graaff accelerator facility of the Australian National

*Email: N.Curtis@bham.ac.uk

†Present address: Department of Chemistry, Indiana University, Bloomington, IN 47405.

‡Present address: Department of Physics, Rutgers University, Newark, NJ 07102.

§Present address: Rudjer Bosković Institute, Department of Experimental Physics, Bijenicka 54, HR-10000 Zagreb, Croatia.

University. A 58 MeV ^{7}Li beam was used to bombard a nominally 100 μg/cm^2 lithium oxide (Li_2O) target supported by an 8 μg/cm^2 ^{12}C backing. Previous work [9] using Similar targets produced by the same evaporation process has indicated, however, that the target composition may well have been closer to $LiCO_4$. Hence the total carbon content was likely to have been greater than 8 μg/cm^2. The integrated beam exposure for the experiment was 0.3 mC.

The particles emitted in the decay of ^{10,11,12}B* were detected in coincidence in an array of four (50 $\times$ 50 mm) detector telescopes. The first element in each telescope was a 70 μm thick silicon ΔE detector, segmented into four independent (25 $\times$ 25 mm) quadrants. The second element was a 500 μm thick silicon strip detector. This was segmented into 16 independent (50 $\times$ 3 mm) resistive strips, each providing position information along the strip length with a resolution of $\sim$0.3 mm. The energy resolution for 34 MeV ^{7}Li ions elastically scattered from Au was 190 keV. The third element in each telescope was a 10 mm thick CsI scintillator. Used in combination, the three detectors comprising each telescope provided energy and position information as well as particle identification for all isotopes from ^{1}H to ^{9}Be. Two telescopes were positioned horizontally (denoted in-plane) either side of the beam axis at center angles of 18° and at a target to strip detector distance of 135 mm. For these detectors, the strips of the silicon strip detectors were horizontal. The remaining two telescopes were placed vertically above and below the beam axis (denoted out-of-plane) at center angles of 28° and at a distance of 140 mm. For these detectors, the strips were vertical.

III. EXPERIMENTAL RESULTS

The various stages of the data analysis are outlined below. Example spectra are given for events where the detected breakup fragments were an α particle and a ^{7}Li resulting from the breakup of ^{11}B following interactions with the ^{7}Li content of the target. These steps were followed for all of the decay channels studied, however. Breakup was observed from the ^{7}Li, ^{12}C, and ^{16}O content of the target.

The α+Li and H+Be fragments arising from the decay of excited states in ^{10,11,12}B were identified using the ΔE-E information provided by the detector telescopes. Figure 1 shows a telescope particle identification (PI) spectrum, which is a plot of the energy deposited in the 70 μm thick silicon ΔE detector against that in the 500 μm thick silicon strip detector. In this spectrum, the isotopes p, d, t, ^{3,4,6}He, ^{6,7,8}Li, and ^{7,9}Be are observed. Figure 2 shows a second PI spectrum obtained from the silicon strip detector and CsI scintillator signals. The isotopes p, d, t, and ^{4}He are clearly observed in this spectrum. These events correspond to those in which highly energetic particles, with sufficient energy to pass through both of the silicon detectors, were incident on the telescope. For each reaction channel studied, the decay products of interest were selected using software windows drawn around the particle loci in the PI spectra.

To study reaction channels involving decay to the ^{8}Be ground state (which is unbound to 2α decay by 93 keV),

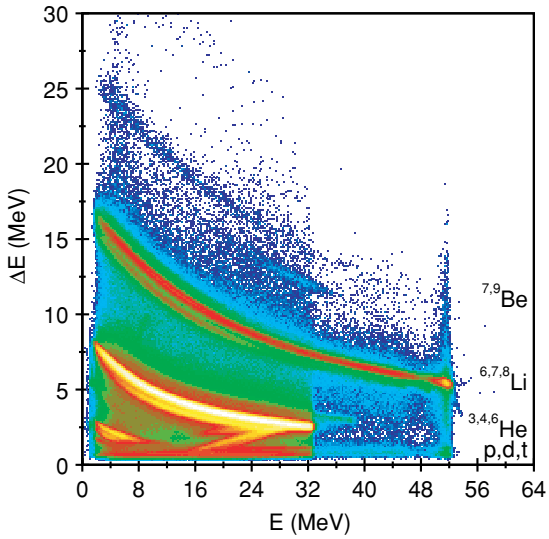

FIG. 1. (Color online) PI spectrum obtained from the 70 μm thick silicon (ΔE) and 500 μm thick silicon strip (E) detectors in a single telescope.

events were selected in which two α particles were detected in coincidence in a single detector telescope. The ^{8}Be ground state was identified by reconstructing the relative energy $E_{\rm rel}$ [10] between the α particles and by selecting those events appearing at an $E_{\rm rel}$ equal to the decay Q value Q_2, of 93 keV. An example relative energy spectrum is shown in Fig. 3. In this spectrum, a clear peak is seen at $E_{\rm rel} = 93$ keV; these events correspond to the 2α decay of the ^{8}Be ground state. A similar analysis was performed during the reconstruction of the α+d decay of the 2.185 MeV, 3$^+$ state in ^{6}Li.

To select the various decay channels of interest, Q-value spectra were produced for each reaction by summing the energies of the two detected fragments (E_1 and E_2) with that of the undetected recoiling particle $E_{\rm rec}$. The total energy in

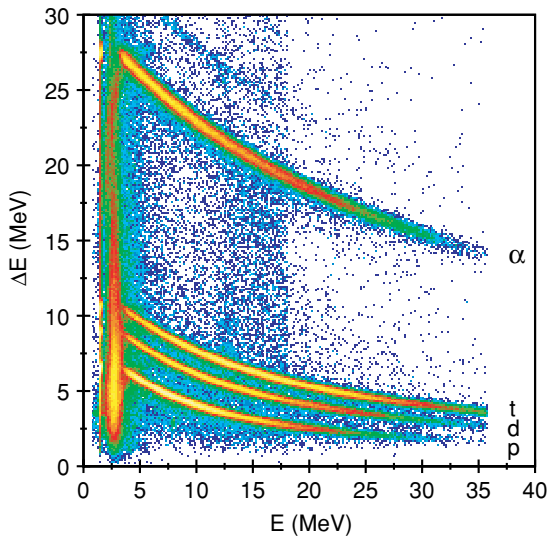

FIG. 2. (Color online) PI spectrum obtained from the 500 μm thick silicon strip (ΔE) and CsI scintillator (E) detectors in a single telescope.

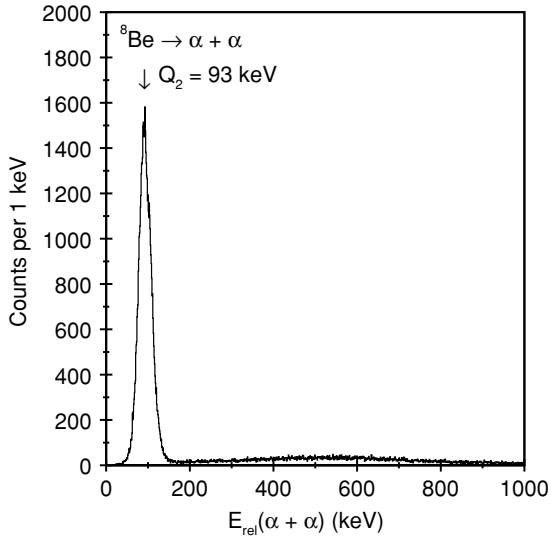

FIG. 3. $E_{\rm rel}$ spectrum for double α particle hits in a single detector telescope. Predicted position of events corresponding to the 2α decay of the ^{8}Be ground state is indicated at 93 keV.

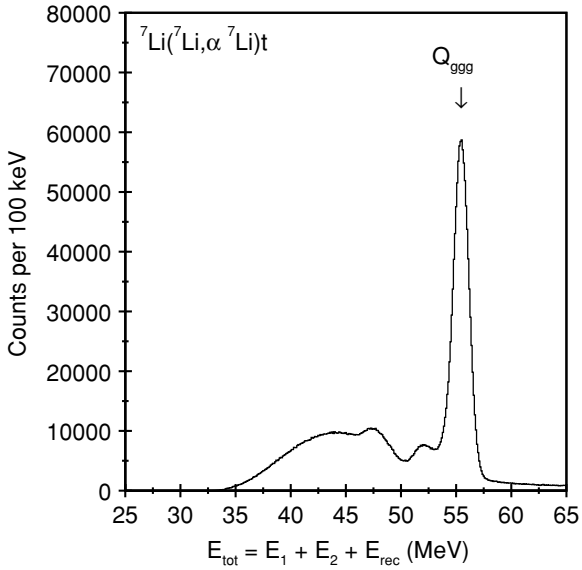

FIG. 4. $E_{\rm tot}$ spectrum for the ^{7}Li(^{7}Li,α ^{7}Li)t reaction.

the exit channel, $E_{\rm tot} = E_1 + E_2 + E_{\rm rec}$, is equal to the sum of the beam energy and the three-body Q value for the reaction, $E_{\rm tot} = E_{\rm beam} + Q_3$ [10]. The recoil energy was determined in each case from the missing momentum between the beam and two detected particles, $\mathbf{p}_{\rm rec} = \mathbf{p}_{\rm beam} - \mathbf{p}_1 - \mathbf{p}_2$, and by making an assumption of the recoil mass ($m_{\rm rec}$). Any misidentification of a detected particle (due to, for example, poor PI resolution) will lead to both an incorrect momentum calculation for that fragment and an incorrectly assumed recoil mass. This will in turn lead to an incorrect $E_{\rm tot}$ value, such that misidentified reactions will be shifted in the $E_{\rm tot}$ spectrum.

Figure 4 shows a typical $E_{\rm tot}$ spectrum, in this case for the ^{7}Li(^{7}Li,α ^{7}Li)t reaction. The strong peak at $E_{\rm tot} =$ 55.4 MeV, labeled $Q_{\rm ggg}$, corresponds to this reaction channel with all three final state particles being emitted in the ground state. For this reaction $Q_3 = -2.467$ MeV, and hence the predicted position of the $Q_{\rm ggg}$ peak is 55.533 MeV. The slight difference between the predicted and observed energies arises from the energy loss of the beam and decay particles within the target and the uncertainty in the target thickness. The additional peaks in Fig. 4 at $E_{\rm tot} \sim$ 52.0 and 47.4 MeV correspond to the ^{16}O(^{7}Li,α ^{7}Li)^{12}C and ^{16}O(^{7}Li,α ^{7}Li)^{12}C$*$[4.43 MeV, 2^+] channels, respectively. The background at $E_{\rm tot}$ 45 MeV corresponds to events where one (or more) of the detected particles has been misidentified or to 4 (or more) body reactions.

The contribution from the ^{16}O content of the target may be seen more clearly in Fig. 5. This is in effect a plot of the recoil energy determined from energy conservation ($E_{\rm rec} - Q_3 = E_{\rm beam} - E_1 - E_2$) plotted against that determined from momentum conservation ($E_{\rm rec} = \mathbf{p}^2_{\rm rec}/2$). Note, however, that the recoil energy should be given by $\mathbf{p}^2_{\rm rec}/2m_{\rm rec}$. As the recoil mass has not been included in the calculation, this spectrum is strictly a plot of the recoil energy determined from energy conservation (in MeV) plotted against the recoil energy times the recoil mass determined from momentum conservation (in MeVu, where u is the atomic mass unit). Hence $Q_{\rm ggg}$ events will appear in the spectrum as a locus with a slope given by $1/m_{\rm rec}$ and an intercept on the $E_{\rm rec} - Q_3$ axis equal to $-Q_3$. Spectra such as this are useful for identifying the recoil (and therefore target) mass in cases when the target is not composed of a single isotope (such as in the present work). In Fig. 5, the detected particles were α and ^{7}Li. In this spectrum, the $Q_{\rm ggg}$ events from the ^{7}Li(^{7}Li,α ^{7}Li)t reaction will lie on a line with a slope of $1/m_{\rm rec} = 1/3$ and an intercept equal to $-Q_3 =$ 2.467 MeV. The solid line indicates the predicted location of these events. The dashed line indicates events from the ^{16}O(^{7}Li,α ^{7}Li)^{12}C reaction, and the dotted line the ^{16}O(^{7}Li,α ^{7}Li)^{12}C$*$[4.43 MeV, 2^+] channel. The two lines from the ^{16}O content of the target each have a slope of $1/m_{\rm rec} = 1/12$. Placing software windows around the events with a slope of

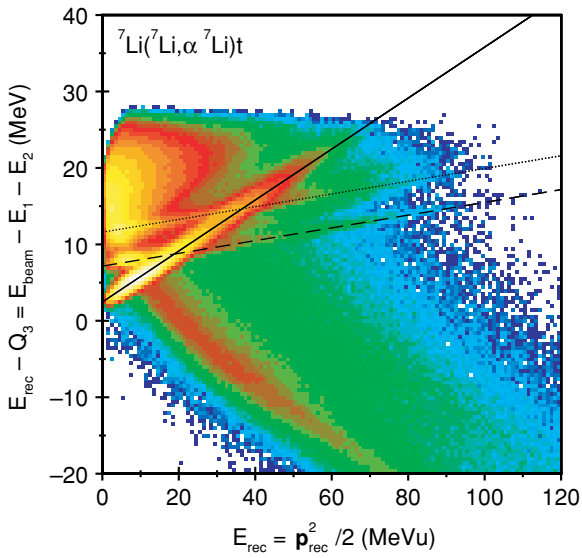

FIG. 5. (Color online) $(E_{\rm rec} - Q_3)$ vs $\mathbf{p}^2_{\rm rec}/2$ for the ^{7}Li(^{7}Li,α ^{7}Li)t reaction. Predicted $Q_{\rm ggg}$ locus is indicated by the solid line (see text).

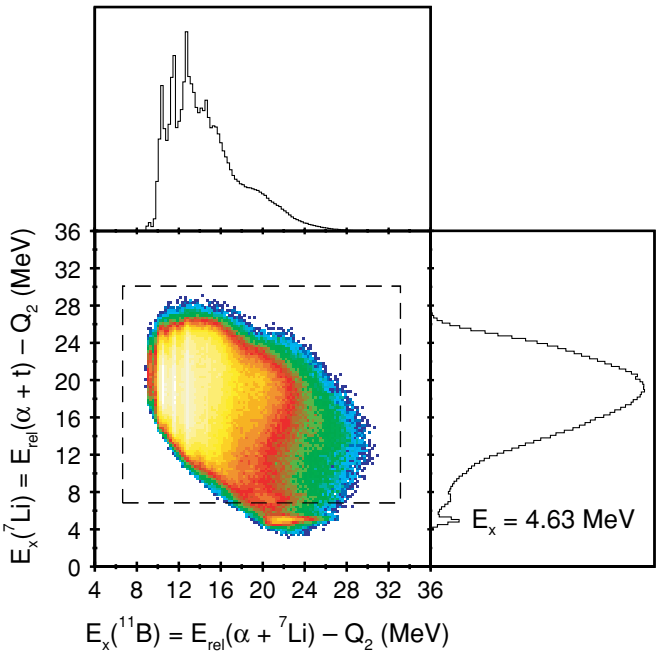

FIG. 6. (Color online) Excitation energy for the α+^{7}Li breakup of ^{11}B plotted against that for the α+t breakup of ^{7}Li. Dashed box indicates the region used to gate out the strong state at 4.63 MeV in ^{7}Li.

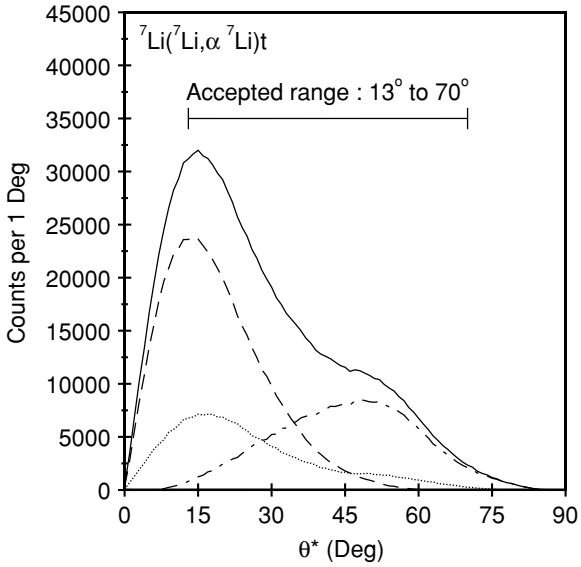

FIG. 7. Excited ^{11}B c.m. scattering angle θ^* distribution obtained from the ^{7}Li(^{7}Li,α ^{7}Li)t reaction.

1/3 allowed the ^{7}Li(^{7}Li,α ^{7}Li)t channel to be selected and the events arising from the oxygen content of the target to be rejected.

After selection of the ^{7}Li(^{7}Li,α ^{7}Li)t events, the relative energy between the detected α and ^{7}Li was used to determine the excitation energy (E_x) in the decaying ^{11}B parent nucleus via $E_x = E_{\text{rel}} - Q_2$ (Q_2 being the breakup Q value) [10]. This was plotted against the excitation energy in ^{7}Li determined from the detected α particle and the undetected (reconstructed) triton recoil. This spectrum is shown in Fig. 6. The horizontal locus of events at $E_x(^7\text{Li}) \sim 4.8$ MeV corresponds to the α+t decay of the 4.63 MeV state in ^{7}Li. This has been labeled in the projection onto the $E_x(^7\text{Li})$ axis. The vertical lines [seen more clearly in the projection onto the $E_x(^{11}\text{B})$ axis] arise from the α+^{7}Li decay of a number of excited states in ^{11}B. There is no evidence for diagonal loci corresponding to the ^{7}Li+t decay of ^{10}Be. By selecting events within the dashed box shown in Fig. 6, the background contribution from the α+t decay of ^{7}Li was removed from the ^{11}B excitation energy spectrum.

To compare the relative decay strengths of the various breakup reactions studied in ^{10,11,12}B, a gate was applied to the data from each channel to ensure that the same θ^* range was sampled. This angle θ^* is the c.m. scattering angle of the excited boron nucleus [10] and is determined by considering the C.M. angle of the reconstructed recoil in the initial two-body reaction. An example θ^* distribution is shown in Fig. 7. This was obtained by determining the scattering angle of the t recoil in the ^{7}Li(^{7}Li,α ^{7}Li)t channel. As the recoil is produced in the initial ^{7}Li(^{7}Li,^{11}B*)t two-body reaction, the θ^* distribution for the t recoil must mirror that of the scattered ^{11}B* (as the t and ^{11}B* are produced back to back in the c.m. frame). The solid line in Fig. 7 indicates the θ^* distribution for all decays to the ^{7}Li(^{7}Li,α ^{7}Li)t channel for all ^{11}B excitation energies. The dashed line is for those events detected in the in-plane pair of detector telescopes, the dotted line is for the out-of-plane telescope pair, and the dot-dash line is for coincidences between one in-plane and one out-of-plane telescope (diagonal coincidences). It can be seen that the shoulder in the total distribution (solid line) between 45° and 60° results from the large efficiency for detecting diagonal coincidences in this region and is not an effect of oscillations in the angular distribution. The variation in θ^* coverage with ^{11}B excitation energy (E_x) has been examined by producing θ^* spectra, similar to that shown in Fig. 7, for 1 MeV wide excitation energy bins over the range to which the current data are sensitive (E_x = 9 to 26 MeV, see below). The variation in θ^* coverage with excitation energy was found to be minimal.

The total θ^* distribution seen in Fig. 7 covers the range 0° to 87°. However, only events in the 13° to 70° range have been accepted. This limiting range corresponds to that covered in one of the other ^{11}B decay channels studied, ^{7}Li(^{7}Li,d ^{9}Be)t (for the third ^{11}B decay channel studied, ^{7}Li(^{7}Li,t ^{8}Be)t, the θ^* range covered was found to be 5° to 97°). Limiting all three of the ^{11}B decay channels to the same θ^* range allowed an accurate comparison of the relative decay strengths for d, t, and α decay to be made (as any variations in the region of the angular distribution sampled will have been removed). A similar analysis was performed separately for the various decay channels studied in both ^{10}B and ^{12}B.

The excitation energy spectra obtained for ^{10}B, ^{11}B, and ^{12}B following the analysis procedures described above are shown in Figs. 8, 9, and 10, respectively. In Fig. 8, the ^{10}B E_x spectra were obtained from the ^{12}C content of the target, whereas the ^{11}B and ^{12}B data in Figs. 9 and 10 are from the ^{7}Li content. In each case, the experimental detection efficiency for the decay channel is indicated by the dotted line, and the peak

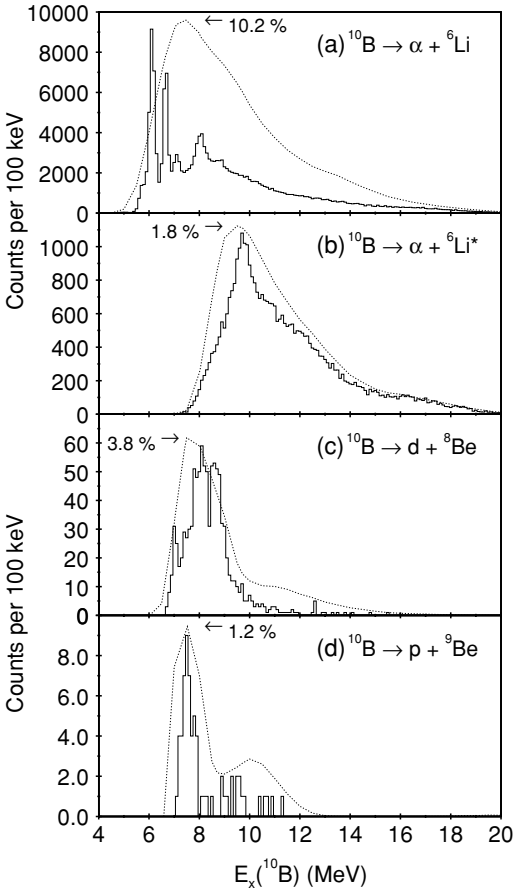

FIG. 8. Excitation energy spectra for the decay of ^{10}B. Dotted lines indicate the experimental detection efficiencies for the channels. Peak detection efficiencies are noted.

efficiency is noted. The efficiencies were obtained from a Monte Carlo code that simulated the two-body reaction that resulted in the production of the excited boron nucleus (for example, the ^{7}Li(^{7}Li,^{11}B*)t reaction), the sequential decay of that nucleus into the decay fragments (for example, the decay of ^{11}B* into α+^{7}Li) assuming an isotropic c.m. distribution, and the detection of the fragments in the detector telescopes. The detection of the fragments was simulated both with angular cuts to mimic the solid angles covered by the telescopes and with energy cuts to simulate the detection thresholds of the various detector elements within the telescopes themselves. The Monte Carlo code used a random number generator that reproduced the experimentally determined θ^{*} distribution measured in the α-decay channel for the particular boron isotope being studied. This random number generator was then used for all of the simulations for the other decay channels of that isotope. For example, the simulation performed to produce the efficiency profile for the d+^{9}Be decay of ^{11}B [Fig. 9(c)] used the random number generator written to reproduce the ^{11}B θ^{*} distribution measured in the α+^{7}Li decay channel (shown in Fig. 7). This was necessitated by the poor statistics in the p, d, and t-decay channels which prevented the accurate determination of the θ^{*} distributions in these cases (although the θ^{*} distributions should in fact be identical because the

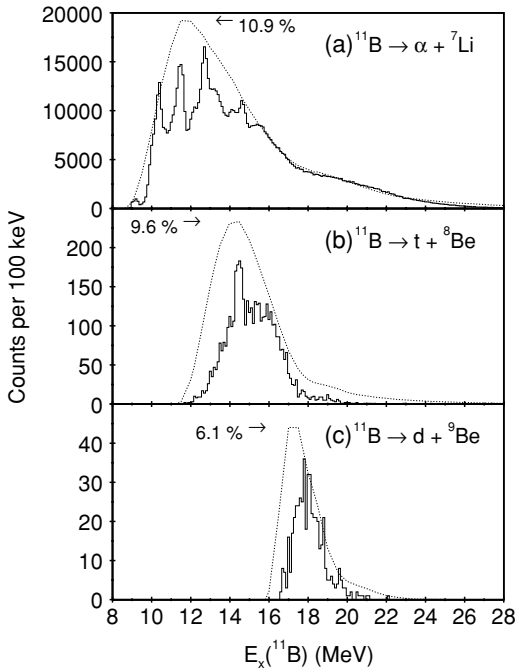

FIG. 9. Same as Fig. 8, but for ^{11}B.

production of the excited ^{11}B nucleus occurs sequentially before, and is therefore independent of, the decay).

In the excitation energy spectra shown in Figs. 8, 9, and 10, several examples can be seen where channels with similar detection efficiencies have markedly different observed yields, even though the same θ^{*} range was sampled in the analysis. One example is seen in Fig. 10, where the decay to the α+^{8}Li and t+^{9}Be channels have similar peak efficiencies (8.7% and 11.6%, respectively), but vastly different yields [approximately 2000 counts per 100 keV maximum in Fig. 10(a) and 60 counts per 100 keV maximum in Fig. 10(b)]. This is an indication of the difference in the cross sections for the ^{7}Li(^{7}Li,α ^{8}Li)d and ^{7}Li(^{7}Li,t ^{9}Be)d reaction channels and suggests that the α decay of ^{12}B has a much larger

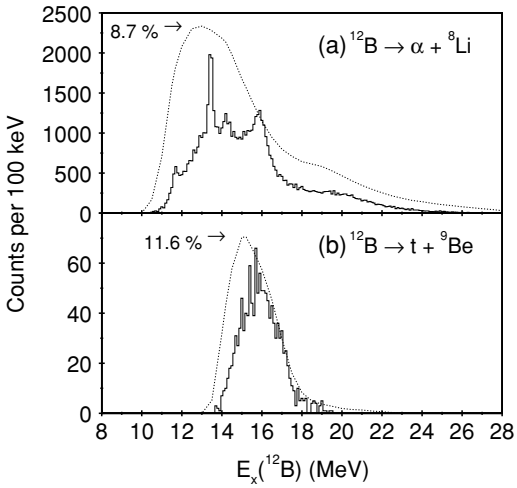

FIG. 10. Same as Fig. 8, but for ^{12}B.

TABLE I. Excitation energies, decay channels, and relative yields for the states observed in ^{10}B from the ^{12}C content of the target. The relative yield is given for those states observed to decay to more than one channel in the present work. Relative yield upper and lower limits have been obtained from Monte Carlo simulations (see text).

E_x (MeV)		Channel	Relative yield (%)
Ref. [11]	Present		
6.127	6.12	α+^{6}Li	
6.560	6.66	α+^{6}Li	
7.002	7.09	α+^{6}Li	88.5 ± 4.1
	7.03	$d+^8$Be	11.5 ± 1.5
7.480, 7.560	7.52	$p+^9$Be	80.2 ± 9.8
	(7.41)	$d+^8$Be	19.8 ± 6.7
8.070	8.04	α+^{6}Li	91.1 ± 2.5
	8.01	$d+^8$Be	8.9 ± 1.0
8.680	8.72	α+^{6}Li	86.5 ± 6.2
	8.71	$d+^8$Be	13.5 ± 1.7
9.580	9.72	$p+^9$Be	<2.4
	9.72	$d+^8$Be	<1.1
	9.72	α+^{6}Li	<7.1
	9.72	α+^{6}Li*	>89.4

branching ratio than the t decay. The measurement of the relative decay strengths for the decay of ^{10,11,12}B to the various decay channels studied is described below.

Each of the excitation energy spectra shown in Figs. 8–10 has been fitted using a smoothly varying polynomial background and Gaussian peak shapes. Each fit was performed a minimum of five times using different background polynomial orders, number of peaks fitted, and varying background ranges. An average was taken of all fits to obtain accurate peak centroids and areas. The counts in each peak were efficiency corrected using the Monte Carlo predicted efficiencies described above to obtain yields for each state. Where the decay of a particular state was observed in more than one channel, the relative yields were then calculated. The fitted centroid energies and relative yields for the decay of ^{10}B observed from the ^{12}C content of the target (Fig. 8) are given in Table I. In Table II the results for ^{10}B decay observed from the target ^{16}O content (excitation energy spectra not shown) are given. These are consistent with the ^{12}C results. Tables III and IV are for ^{11}B (Fig. 9), and ^{12}B (Fig. 10), respectively. The uncertainties quoted in the relative yields arise from statistical uncertainties in the peak areas. The centroid statistical uncertainties are 20 keV or less. Systematic uncertainties are expected to be 200 keV.

In Tables I, II, III, and IV, relative decay strengths are given for all states that have been observed to decay to more than one channel. However, there are a number of cases in which a state is seen in one decay channel only, despite the detection efficiencies for the other channels studied being nonzero at the particular excitation energy of that state. One example is the 9.72 MeV state in ^{10}B (Table I), which is only observed in the α+^{6}Li*[2.185 MeV, 3$^+$] channel. There is no evidence for this state in either the $\alpha+^6\mathrm{Li}_{gs}$, d+^{8}Be, or

TABLE II. Same as Table I, but for the states observed in ^{10}B from the ^{16}O content of the target.

E_x (MeV)		Channel	Relative yield (%)
Ref. [11]	Present		
4.774, 5.110	4.97	α+^{6}Li	
6.127	6.10	α+^{6}Li	
6.560	6.66	α+^{6}Li	
7.002	7.10	α+^{6}Li	93.4 ± 8.4
	(7.30)	$d+^8$Be	6.6 ± 1.3
7.480, 7.560	(7.60)	p+^{9}Be	
8.070	8.05	α+^{6}Li	94.3 ± 16.2
	(7.97)	$d+^8$Be	5.7 ± 1.4
8.680	8.50	α+^{6}Li	94.5 ± 19.4
	8.78	d+^{8}Be	5.5 ± 1.1
9.580	9.87	p+^{9}Be	<14.8
	9.87	d+^{8}Be	<6.4
	9.95	α+^{6}Li	<26.8
	(9.80)	α+^{6}Li*	>52.0

TABLE III. Same as Table I, but for the states observed in ^{11}B.

E_x (MeV)		Channel	Relative yield (%)
Ref. [11]	Present		
9.185	9.18	α+^{7}Li	
10.330	10.36	α+^{7}Li	
11.265	11.42	α+^{7}Li	
12.557	12.65	α+^{7}Li	>99.8
	12.65	t+^{8}Be	<0.2
13.137, 13.160	13.21	α+^{7}Li	>99.8
	13.21	t+^{8}Be	<0.2
14.340, 14.565	14.64	α+^{7}Li	97.7 ± 8.3
	14.46	t+^{8}Be	2.3 ± 0.2
15.290	15.62	α+^{7}Li	96.7 ± 10.6
	(15.40)	t+^{8}Be	3.3 ± 0.6
	(17.60)	d+^{9}Be	>69.0
	(17.76)	t+^{8}Be	<31.0
	(18.31)	d+^{9}Be	>81.9
	(18.25)	t+^{8}Be	<18.1
	(19.63)	d+^{9}Be	>65.2
	(19.51)	t+^{8}Be	<34.8

TABLE IV. Same as Table I, but for the states observed in ^{12}B.

E_x (MeV)		Channel	Relative yield (%)
Ref. [11]	Present		
11.590	11.67	α+^{8}Li	
13.330	13.44	α+^{8}Li	
(14.1)	14.20	α+^{8}Li	>94.9
	14.20	t+^{9}Be	<5.1
15.5	15.90	α+^{8}Li	99.6 ± 4.2
	(15.87)	t+^{9}Be	0.4 ± 0.2

p+^{9}Be channels, even though these channels have detection efficiencies of 6.41%, 0.89% and 0.32% respectively, at this energy (for α+^{6}Li*[2.185 MeV, 3$^+$] the efficiency is 1.75%). In these cases, the decay to the unobserved channels has been simulated using a Monte Carlo code designed to reproduce the experimental excitation energy resolution in breakup reactions [13]. For the example given above, the code initially simulates the two-body reaction ^{12}C(^{7}Li,^{10}B*)^{9}Be with an excitation energy of 9.72 MeV. The decay of ^{10}B* at 9.72 MeV to the channel of interest is then simulated (the code is used for each of the three decay channels in turn), and the laboratory energies and angles of the decay fragments are calculated. These are then altered to simulate various physical effects, such as particle energy loss, energy straggle, and angular straggle in the target, and detector position and energy resolutions. This is performed by adding (or subtracting) an energy (or angle) obtained from a Gaussian random number generator centered at zero. The width of the Gaussian is obtained from estimates of the magnitude of the effect to be simulated (for the example of detector energy resolution this would be 190 keV, as noted in Sec. II). The Monte Carlo events are then analyzed in the same way as the real experimental data, and an excitation energy spectrum produced. Due to the smearing of the particle energies and angles, the reconstructed excitation energy will not exactly equal the energy simulated by the code (in this example, 9.72 MeV), but it will have a (typically) Gaussian shape, centered at 9.72 MeV and with a width indicative of the experimental resolution (for the α+^{6}Li channel, for example, this is 320 keV). The Monte Carlo code can therefore produce pseudoevents that can be used to mimic real events, even if the decay channel simulated was not actually observed in the experiment.

The pseudoevents produced by the Monte Carlo code have been used to determine upper limits for the relative decay strengths for the unobserved channels discussed above. This analysis was performed by adding Monte Carlo events to the experimentally obtained excitation energy spectra for the decay channels of interest [for the example, given these are α+^{6}Li$_{gs}$, d+^{8}Be, and p+^{9}Be at E_x(^{10}B) = 9.72 MeV]. Monte Carlo events were added to the E_x spectra until clear peaks were observed, the number of events required to do this providing an upper limit to the number of real events detected. If, for example, N Monte Carlo events were required to produce an observable peak, then the number of real detected events must be less than N, or otherwise a peak would have been observed in the raw excitation energy spectrum before the Monte Carlo events were introduced. The upper limits to the number of detected events were then used to provide upper limits for the relative decay strengths of the unobserved channels. This procedure was followed for the 9.72 MeV state in ^{10}B (Tables I and II), the 12.56, 13.14, and >16 MeV states in ^{11}B (Table III), and the (14.1) MeV state in ^{12}B (Table IV).

One further analysis step was performed for two of the reaction channels studied. These were subject to possible contamination from decays to excited fragments.

It is possible that the Q_{ggg} peak seen in Fig. 4 contains events from both the ^{7}Li(^{7}Li,α ^{7}Li$_{gs}$)t and ^{7}Li(^{7}Li,α ^{7}Li*[0.478 MeV])t channels. The excitation energy reconstructed for events corresponding to the excited channel will be underdetermined by an energy equal to that carried by the excited fragment (0.478 MeV). To determine the contributions from these two reactions, excitation energy spectra were produced by gating on the upper and lower energy sides of the Q_{ggg} peak. The analysis suggests that the shoulder seen in Fig. 9(a) at 12.18 MeV corresponds to the decay of the 12.65 MeV state to the α+^{7}Li*[0.478 MeV] channel. This is supported by the 0.47 MeV separation of these two features. Similarly, the peak at 14.15 MeV would appear to result from the decay of the state at 14.64 to the excited channel (in this case the separation is 0.49 MeV). The contribution from the ^{7}Li(^{7}Li,α ^{7}Li*[0.478 MeV])t channel appears to be very small for all of the other peaks seen in Fig. 9(a).

A similar analysis was performed for the ^{7}Li(^{7}Li,α ^{8}Li)d reaction, the energy of the first excited state of ^{8}Li being 0.981 MeV. The excitation energy spectra obtained from the upper and lower energy sides of the Q_{ggg} peak observed in the E_{tot} spectrum for this channel were almost identical, suggesting that the contribution to Fig. 10(a) from decay to the α+^{8}Li[0.981 MeV] channel was negligible.

Finally it is noted that a number of the breakup channels discussed above have been observed from more than one element within the target. An example is the α+^{7}Li decay of ^{11}B which is seen (in Fig. 4) from both the ^{7}Li and ^{16}O content. We have only presented the ^{7}Li target results here [Fig. 9(a)]. It would be very difficult to compare the yields to the ^{7}Li(^{7}Li,α ^{7}Li)t and ^{16}O(^{7}Li,α ^{7}Li)^{12}C channels, because the absolute target composition (the relative thicknesses of the ^{7}Li, ^{12}C, and ^{16}O) is unknown. We have therefore only presented the relative decay strengths to the various channels from a single target element, as in this case the absolute thickness of that particular element within the target is not required.

IV. DISCUSSION

The isospin of the decay channels of a state may be used to infer the probable isospin of the state itself. For ^{10}B, both the α+^{6}Li and d+^{8}Be channels correspond to $T = 0$ final states, whereas the unique proton decay of ^{10}B most likely signals the decay of $T = 1$ states. It can be seen that for the ~7.5 MeV state in ^{10}B (Table I) p decay dominates over d decay by approximately 80:20. Thus it is likely that this is the decay of either the 7.48 MeV 2$^-$ or the 7.56 MeV 0$^+$ $T =$ 1 state (or possibly both). However, both the 7.43 MeV 1$^-$ $T =$ 1 and 7.469 MeV 2$^+$ $T = 1$ states are also possible candidates for this decay, making further conclusions difficult.

The 9.72 MeV peak is only observed in the α+^{6}Li* [2.185 MeV, 3$^+$] ($T = 0$) channel and almost certainly corresponds to the 9.58 MeV peak observed in the same decay channel in Ref. [2]. In the earlier measurements, a peak at 7.96 MeV was also observed to decay to the same final state. This lies outside the range of sensitivity of the present work. However, the present measurement can confirm that the peak at (9.7 $\pm$ 0.2) MeV decays most strongly to the α+^{6}Li* [2.185 MeV, 3$^+$] final state. This might suggest a special structure with a large overlap with that of the excited ^{6}Li nucleus.

TABLE V. Comparison between the experimental and calculated deuteron and α width ratios (Γ_d/Γ_α) for ^{10}B, and triton and α width ratios (Γ_t/Γ_α) for ^{11}B. The decay angular momentum $L_{\rm decay}$ is also shown.

	E_x (MeV)		J^π	$L_{\rm decay}$	Width ratios	
	Present	Refs. [11,12]			Expt.	Calc.
^{10}B	7.09	7.002	(3^+)	2	0.130(17)	0.053
	8.04	8.07	2^+	2	0.097(11)	0.235
	8.72	8.68	(3^+)	2	0.156(22)	0.329
^{11}B	12.65	12.557	$1/2^+(3/2^+)$	1:0[a]	<0.0020	0.1457

[a] $L_{\rm decay}(\alpha) : L_{\rm decay}(t)$.

The most dominant decay channel in all three isotopes studied is that of α decay (90–100%). This suggests that the α particle plays an important role in the structure of ^{10,11,12}B and may be seen as strong evidence for α+Li clustering in these nuclei.

In general, a study of the decay strengths for different decay channels may be used as an indicator of the underlying (cluster) structure of the state. In the case of ^{10}B, the relative strength of the $\alpha+^6$Li decay compared with that for $d+^8$Be, given the association of ^{8}Be with an $\alpha+\alpha$ cluster structure, may provide an indication of two- or three-centered cluster states, respectively. An enhanced α-decay probability to the ^{6}Li ground state, compared with that for deuteron decay, would indicate an $\alpha+^6$Li structure. However, the three-body cluster $\alpha+\alpha+d$ would be expected to have similar widths for α and d decay. This is of course difficult to distinguish from a decay that is dominated by phase space. Moreover, calculations of the magnitudes of the d and α widths of such three-centered cluster states are required before definite conclusions can be reached.

For ^{11}B the three decay channels sampled are d, t, and α. No significant yield was observed for proton decay. These decay processes sample $\alpha+^7$Li, $t+^8$Be, and $d+^9$Be final states. An enhanced α decay (compared with t decay) would suggest a two-centered cluster structure, whereas a more equal weighting might favor three-centered states.

An examination of the present data indicates that $\alpha+^6$Li decay dominates in ^{10}B, suggesting that there is little or no evidence for three-body cluster states in the present energy region. However, decay probabilities are very sensitive to decay barriers, and such factors must be considered carefully before conclusions are drawn. To be more precise, we have calculated, where possible, the penetrabilities for the d and α decay through the centrifugal and Coulomb barriers [14]. These calculations were performed with a channel radius of $r = r_0(A_1^{1/3} + A_2^{1/3})$ with $r_0 = 1.4$ fm, and in general they show that d decay is suppressed more than α decay (the decay threshold is higher) by the presence of the barrier. Table V presents the comparison between the experimental Γ_d/Γ_α ratios and those calculated assuming the decay is determined only by the barrier penetrabilities and the statistical weights resulting from the spins of the decay products. This analysis is only possible in the case when states have previously been identified with spin and parity assignments. The table shows two states at 7.002 and 8.68 MeV which have the tentative assignment 3^+ and another at 8.07 MeV assigned 2^+. It is observed for the 8.07 and 8.68 MeV states that the experimental values of Γ_d/Γ_α are approximately half of the calculated values, indicating enhanced α widths. For the 7.002 MeV state, the opposite situation is found, with the deuteron width being enhanced compared with the calculations. This may, however, indicate that the tentative 3^+ assignment is incorrect.

A similar analysis was performed for the 12.557 MeV $1/2^+$ state in ^{11}B (Table V). The comparison between experimental and calculated Γ_t/Γ_α suggests that the α widths are strongly enhanced. This indicates a possible $\alpha+^7$Li cluster structure.

We note that the states observed in the $\alpha+^8$Li decay of ^{12}B are the same as those in Ref. [7]. There are two states that lie above both the α and t decay thresholds at 14.20 and 15.90 MeV in the present work. For these, we observed that α decay is much stronger than t decay, indicating a strong α-cluster structure. However, without a determination of the spins of the states, this cannot be confirmed.

Many similarities exist between the ^{11}B states observed in the present work and those seen in the ^{7}Li(^{9}Be,^{11}Be[$\alpha+^7$Li]) reaction [6]. For example, in both measurements the $K = 5/2^+$ deformed cluster band proposed in [6] is observed, here as the states at 9.185 MeV ($7/2^+$) and 11.265 MeV ($9/2^+$). These states lie below the t-decay threshold, and thus determination of the relative cluster decay widths was not possible in the present measurement. The 12.577 and 14.34 MeV states were also observed in [6] via the same $T = 1/2$ decay channel as in the present measurement. We therefore confirm the observation by Soić *et al.* that these states (listed in Ref. [12]) do not have $T = 3/2$ character (or alternatively that different states are observed at a similar energy to those with $T = 3/2$ character, but have isospin $T = 1/2$). It has been suggested [6] that the 12.577 MeV state is the $9/2^+$ member of the proposed $K^\pi = 3/2^+$ cluster band. For a $9/2^+$ state, Γ_t/Γ_α[calc.] = 0.0008. This value is consistent with the upper limit in the present data.

V. SUMMARY

A study of the (^{7}Li,^{10,11,12}B*) reaction at 58 MeV from the ^{7}Li, ^{12}C, and ^{16}O content of a mixed target has provided the first measurement of the relative decay strengths of the α+Li

and H+Be decay of ^{10,11,12}B. In all three isotopes, the α-decay channel dominates, indicating that α+Li clustering plays an important role in the structure of these nuclei. Firm spin and parity assignments for the states in ^{10,11,12}B above the p, d, t, and α-decay thresholds are required, however, to allow barrier penetrabilities to be calculated to confirm this suggestion.

ACKNOWLEDGMENTS

The assistance of the staff at the Australian National University 14 UD tandem facility is gratefully acknowledged. This work was funded by the United Kingdom Engineering and Physical Sciences Research Council.

[1] Y. Kanada-En'yo and H. Horiuchi, Phys. Rev. C **52**, 647 (1995).
[2] P. J. Leask, M. Freer, N. M. Clarke, B. R. Fulton, C. D. Freeman, S. M. Singer, W. N. Catford, N. Curtis, K. L. Jones, R. L. Cowin, D. L. Watson, R. P. Ward, N. A. Orr, and V. F. E. Pucknell, Phys. Rev. C **63**, 034307 (2001).
[3] N. Soić, S. Cherubini, M. Lattuada, D. Miljanić, S. Romano, C. Spitaleri, and M. Zadro, Fizika (Zagreb) **B12** (2), 153 (2003).
[4] S. Ahmed, M. Freer, J. C. Angélique, N. I. Ashwood, V. Bouchat, W. N. Catford, N. M. Clarke, N. Curtis, F. Hanappe, J. C. Lecouey, F. M. Marqués, T. Materna, A. Ninane, G. Normand, N. A. Orr, S. Pain, N. Soić, C. Timis, A. Unshakova, and V. A. Ziman, Phys. Rev. C **69**, 024303 (2004).
[5] N. Soić, M. Freer, L. Donadille, N. M. Clarke, P. J. Leask, W. N. Catford, K. L. Jones, D. Mahboub, B. R. Fulton, B. J. Greenhalgh, and D. L. Watson, Nucl. Phys. **A738**, 347 (2004).
[6] N. Soić, M. Freer, L. Donadille, N. M. Clarke, P. J. Leask, W. N. Catford, K. L. Jones, D. Mahboub, B. R. Fulton, B. J. Greenhalgh, D. L. Watson, and D. C. Weisser, Nucl. Phys. **A742**, 271 (2004).
[7] N. Soić, S. Cherubini, M. Lattuada, D. Miljanić, S. Romano, C. Spitaleri, and M. Zadro, Europhys. Lett. **63** (4), 524 (2003).
[8] W. von Oertzen, Nuovo Cimento **110A**, (9–10), 895 (1997).
[9] N. Curtis, M. Shawcross, W. N. Catford, B. R. Fulton, N. M. Clark, S. J. Hall, J. T. Murgatroyd, S. P. G. Chappell, R. L. Cowin, G. Dillon, and D. L. Watson, Phys. Rev. C **61**, 064606 (2000).
[10] N. Curtis, A. St.J. Murphy, M. J. Leddy, J. S. Pople, N. M. Clarke, M. Freer, B. R. Fulton, S. J. Hall, G. Tungate, R. P. Ward, S. M. Singer, W. N. Catford, G. J. Gyapong, R. A. Cunningham, J. S. Lilley, S. P. Chappell, S. P. Fox, C. D. Jones, D. L. Watson, P. M. Simmons, R. A. Hunt, A. C. Merchant, A. E. Smith, W. D. M. Rae, and J. Zhang, Nucl. Instrum. Methods A **351**, 359 (1994).
[11] D. R. Tilley, J. H. Kelley, J. L. Godwin, D. J. Millener, J. E. Purcell, C. G. Sheu, and H. R. Weller, Nucl. Phys. **A745**, 155 (2004).
[12] F. Ajzenberg-Selove and J. H. Kelley, Nucl. Phys. **A506**, 1 (1990).
[13] N. Curtis, N. M. Clarke, B. R. Fulton, S. J. Hall, M. J. Leddy, A. St.J. Murphy, J. S. Pople, R. P. Ward, W. N. Catford, G. J. Gyapong, S. M. Singer, S. P. G. Chappell, S. P. Fox, C. D. Jones, D. L. Watson, W. D. M. Rae, and P. M. Simmons, Phys. Rev. C **51**, 1554 (1995).
[14] A. M. Lane and R. G. Thomas, Rev. Mod. Phys. **30**, 257 (1958).